

LETTER

## Excitation-polarization-dependent dynamics of polariton condensates in the ZnO microwire at room temperature

To cite this article: Ziyu Ye *et al* 2022 *J. Phys.: Condens. Matter* **34** 22LT01

View the [article online](#) for updates and enhancements.

### You may also like

- [Exciton-polariton trapping and potential landscape engineering](#)  
C Schneider, K Winkler, M D Fraser *et al.*
- [Room-temperature polariton waveguide effect in a ZnO microwire](#)  
Yanjing Ling, Wei Xie, Liaoxin Sun *et al.*
- [Enhanced second-harmonic generation by Fano resonance of polaritons](#)  
Lin Wu, Yafeng Wang, Liming Liao *et al.*



**IOP | ebooks™**

Bringing together innovative digital publishing with leading authors from the global scientific community.

Start exploring the collection—download the first chapter of every title for free.

## Letter

# Excitation-polarization-dependent dynamics of polariton condensates in the ZnO microwire at room temperature

Ziyu Ye<sup>1</sup> , Fei Chen<sup>1</sup> , Hang Zhou<sup>2</sup>, Song Luo<sup>2</sup>, Fenghao Sun<sup>1</sup> , Zheng Sun<sup>1</sup>, Yuanlin Zheng<sup>3</sup>, Xianfeng Chen<sup>3,4</sup> , Huailiang Xu<sup>1</sup>, Zhanghai Chen<sup>2</sup>, Hui Li<sup>1,\*</sup> and Jian Wu<sup>1,5,6,\*</sup> 

<sup>1</sup> State Key Laboratory of Precision Spectroscopy, East China Normal University, Shanghai 200241, People's Republic of China

<sup>2</sup> Department of Physics, College of Physical Science and Technology, Xiamen University, Xiamen 361005, People's Republic of China

<sup>3</sup> State Key Laboratory of Advanced Optical Communication Systems and Networks, School of Physics and Astronomy, Shanghai Jiao Tong University, Shanghai 200240, People's Republic of China

<sup>4</sup> Collaborative Innovation Center of Light Manipulation and Applications, Shandong Normal University, Jinan 250358, People's Republic of China

<sup>5</sup> Collaborative Innovation Center of Extreme Optics, Shanxi University, Taiyuan, Shanxi 030006, People's Republic of China

<sup>6</sup> CAS Center for Excellence in Ultra-intense Laser Science, Shanghai 201800, People's Republic of China

E-mail: [hli@lps.ecnu.edu.cn](mailto:hli@lps.ecnu.edu.cn) and [jwu@phy.ecnu.edu.cn](mailto:jwu@phy.ecnu.edu.cn)

Received 4 January 2022, revised 24 February 2022

Accepted for publication 15 March 2022

Published 29 March 2022



## Abstract

Based on ZnO microcavities with high quality factors, where the gain medium exhibits confinement of wave packets due to the intrinsically formed whispering gallery microcavity, strong coupling between excitons and cavity photons can be obtained at room temperature resulting in hybrid quasiparticles, e.g. exciton polaritons. In this work, polariton condensation is induced under the non-resonant excitation by linearly polarized femtosecond laser pulses with different polarization directions. The dynamical angle-resolved  $k$ -space spectra of the photoluminescence emission of polariton condensates are measured with sub-picosecond resolution by the self-developed femtosecond angle-resolved spectroscopic imaging technique. Our results show that the ultrafast dynamics of polariton condensation is sensitive to the polarization direction of the excitation pulses which can be explained qualitatively by the combined effect of selective excitation of distinct exciton modes in the sample and the

\* Authors to whom any correspondence should be addressed.

effective coupling strength of the excitation pulses in the ZnO microcavity for various polarization directions. This work strengthened the understanding of the condensation process for cavity exciton polaritons at room temperature.

Keywords: exciton polariton, ultrafast dynamics, polarization-dependence

(Some figures may appear in colour only in the online journal)

## 1. Introduction

It is known that in the bosonic systems, when the interparticle distance is smaller than the de Broglie wavelength, the particles can spontaneously accumulate in the ground state, forming Bose–Einstein condensation (BEC). BEC was first observed in cold rubidium atoms in 1995 [1]. However, the extreme conditions to achieve atomic BEC are harsh, e.g. ultralow temperatures in the nanoKelvin ( $10^{-9}$  K) level are usually required. Recently, a new state of matter has shown advantages to achieve BEC at high or even room temperature. Exciton–polariton (EP) is a bosonic quasiparticle formed by the strong coupling between excitons and cavity photons in semiconductors [2]. Polariton’s photonic component contributes to its small effective mass, about eight orders of magnitude smaller than that of an atom, which means BEC can be obtained in EPs at high temperatures [3]. The long range spatial and temporal correlation as well as phenomena such as condensation, vortices, and superfluidity have been realized in polaritonic systems [4–8]. So far, experimental studies have focused on static state measurements or exciton dynamics [9], and the highest time resolution is in the order of picosecond [4, 10, 11]. Nevertheless, room-temperature polariton condensates have shown broad potential in applications of compact polaritonic devices where exploration of the ultrafast dynamics is yet in urgent need.

ZnO is one kind of semiconductor with a direct bandgap of 3.37 eV at room temperature. The large exciton binding energy of 60 meV and a large oscillator strength make ZnO a good candidate for the realization of polariton condensation at room temperature [12–16]. The ZnO microwires grown by the chemical vapor deposition (CVD) method intrinsically form whispering-gallery (WG) microcavities with quality factors ( $Q$  factors) above 1000 [17]. The coupling efficiency of photons and excitons can be dramatically enhanced in these WG microcavities. Polariton LED, and polariton lasing in the ultraviolet region have been realized in ZnO WG microcavities [18, 19]. However, the exploration of underlying dynamics of the related polariton condensation process is not sufficient. One major issue is the short lifetime of the polaritons at room temperature, which requires experimental resolution at sub-picosecond time scale that cannot be achieved with commercial streak cameras.

Based on the fact that the coherence of the ensemble is reconstructed during the polariton condensation process, it is

found that the observed condensation signal represents intrinsic features in polarization [20, 21]. Nevertheless, the dependence on the polarization direction of the pumping pulses has been rarely explored. In the present work, linearly polarized femtosecond laser pulses at 350 nm are used for the non-resonant excitation of polariton condensates in a ZnO WG microcavity at room temperature. The angle-resolved  $k$ -space spectra of polariton condensates are measured explicitly with femtosecond resolutions using self-developed techniques [22]. Clear excitation polarization dependence can be recognized in the dynamics of polariton condensation. It is found that when the microcavity is excited with the polarization direction perpendicular to its  $c$ -axis, the polaritons are formed the most efficiently accompanying with the fastest dynamics. The excited particle density monochromatically decreases when the polarization direction rotates towards the  $c$ -axis. Besides the possible coupling efficiency of the excitation pulses into the ZnO microwire, the selective excitation of different species of excitons is found to be responsible for the observed polarization-dependent dynamics.

## 2. Experimental materials and methods

In our experiment, the ZnO WG microcavity (with the diameter in the range of about 2–4  $\mu\text{m}$  and the length over 100  $\mu\text{m}$ ) is grown along the  $c$ -axis by the CVD method. Femtosecond pulses (central wavelength at about 800 nm, pulse duration of around 35 fs, repetition rate at 1 kHz) obtained from a Ti:sapphire amplification system (Coherent Astrella) are sent to a parametric amplifier (TOPAS Prime) for frequency conversion. The output femtosecond pulses at 350 nm are focused onto the ZnO microcavity by an 15 $\times$  objective (Thorlabs, LMU-15X-UVB) to excite polaritons nonresonantly. The laser spot is about 4  $\mu\text{m}$  in diameter. The pulse duration of the excitation pulses is estimated to be around 240 fs (full width at half maximum, FWHM) at the interaction region. The polarization directions of the excitation pulses are controlled by a half-wave plate mounted on a motorized rotational stage. The  $k$ -space photoluminescence (PL) emission is measured by the angle-resolved fluorescence spectrum system [23], and the resulting distributions are detected by a spectrometer (Andor, SR-500i-B1) implementing a two-dimensional intensified charge-coupled detector (ICCD, iStar). In addition, a beam of 35 fs pulses centered at 800 nm with pulse energy of approximately 200  $\mu\text{J}$  are used as the gating pulses applied on a piece of fused silica placed at a focusing plane along the PL light path. Ultrafast gating can be realized based on optical

Kerr effect in the medium. The timing of the gating pulse is precisely controlled using a high-precision motorized delay stage. In this femtosecond angle-resolved spectroscopic imaging (FARSI) technique, the distributions of the PL emission in both the energy and the momentum degrees of freedom can be detected with femtosecond resolutions [22]. All the measurements are carried out for transverse electric (TE) mode emission.

### 3. Results and discussions

The linearly polarized excitation pulses at 350 nm can efficiently produce polariton condensates in ZnO WG microcavity as long as a certain threshold is reached. The power dependence of the ground-state occupancy is measured for different polarization directions of the excitation pulses. The results are shown in figure 1. The ground-state occupancy shows a linear increase with respect to the pumping power below the threshold. It starts to increase nonlinearly at the onset of condensation. This nonlinear region is usually accompanied with strong inter-particle interactions and can be characterized by a linewidth narrowing. The population dependence returns to a linear dependence after this transition region [5, 6]. The point of the first inflection of each curve indicates the corresponding threshold power for polariton condensation. According to figure 1, it can be found apparently that the threshold power exhibits difference for various excitation polarization directions. As the polarization changes from along 0 degree to 90 degree (where 0/90 degree represents the polarization direction perpendicular/parallel to the  $c$ -axis, as shown in the inserted figure in figure 1), the thresholds are obtained at about  $0.52 \mu\text{W}$  (0 degree),  $0.56 \mu\text{W}$  (30 degree),  $0.61 \mu\text{W}$  (60 degree), and  $0.66 \mu\text{W}$  (90 degree), respectively. Accordingly, at a certain excitation power, e.g. at about  $0.6 \mu\text{W}$ , polariton condensation can be achieved for the 0 degree polarization, but not for the polarization directions along 60 and 90 degree. It is verified by this measurement that to achieve the same amount of ground-state occupancy, the required excitation power is increasing for the polarization directions rotating away from 0 degree. As the pump power increases, larger amount of polaritons accumulate at the ground state, leading to stronger interactions. Power-dependent blue shifts can be observed in various polarization conditions.

The dispersion relation of the polaritons can be obtained by using angle-resolved  $k$ -space spectroscopy. Generally, the dispersion curves of multiple lower polariton (LP) branches can be observed for ZnO microwire below the condensation threshold [23]. Whereas above the threshold, polariton condensates will suddenly accumulate on the ground-state of a certain LP branch where the effective quality factor is optimized [17]. Figures 2(a)–(c) present the static-state  $k$ -space angle-resolved PL distributions with different polarization directions along 0, 45, and 90 degree for the same pumping power of  $0.8 \mu\text{W}$ . Polariton condensates at the bottom of the dispersion curve with  $N = 43$  are obtained for all the three polarization directions, where the dispersion curves (indicated by the white dashed curves) are obtained from the fitting results using the classical plane waves model [24]. In the comparison of the

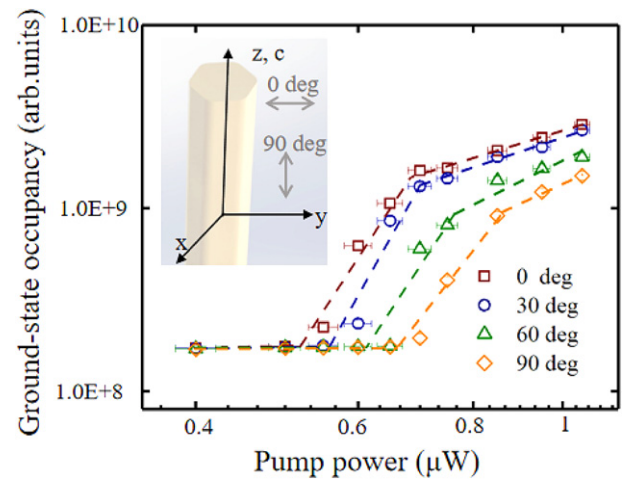


**Figure 1.** The ground-state occupancy vs pump power for polarization directions along 0, 30, 60 and 90 degree, respectively. Corresponding condensation threshold powers are found to be around  $0.52 \mu\text{W}$ ,  $0.56 \mu\text{W}$ ,  $0.61 \mu\text{W}$  and  $0.66 \mu\text{W}$ . Inserted figure: sketch of the ZnO WG microcavity and the coordinates. The pump pulses are along the  $x$  axis. 0/90 degree polarization is along the  $y/z$ -axis. The crystallographic axis ( $c$ -axis) is along the  $z$ -axis.

integrated condensation signal for various polarization directions (shown in figure 2(d)), it is shown that as the polarization direction changes from 0 degree to 90 degree, the intensity of condensates follows a linearly decreasing trend, indicating a monochromatic reduction of the particle densities in the polariton condensates. The polariton condensates also show a red shift in energy when the polarization direction changes from 0 to 90 degree.

To reveal the underlying mechanism of the excitation polarization dependence of polariton condensates, FARSI technique is used to measure the condensation dynamics for different pumping polarization directions at about  $0.85 \mu\text{W}$ . Figures 3(a)–(d) show the angle-integrated PL distributions as a function of energy and delay time for four distinct polarization directions. A dynamical red shift of the condensation is observed for each scan, which can be attributed to the decay of the particle density. Showing in figure 3(e), the slower red shift at larger polarization angle is due to the fact that the lower intensity of condensates results in a reduction in the polariton–polariton interaction. When we compare the time-integrated spectra obtained at different excitation polarization directions (as shown in figure 3(e)), slight red shift can be recognized as the polarization direction rotates from 0 degree to 90 degree, which can be an indication of the variation in the overall occupation density. From these scans, lifetimes of a few picoseconds can be extracted for the EPs in ZnO WG microcavity at room temperature.

The dynamics of polariton condensation can be clearly verified by the time-dependent results. The data presented in figure 3(f) are obtained by integrating the signals shown in figures 3(a)–(d) for the related energies, and the results are compared with the calculations based on rate equations. In our simulation, the arriving excitation pulses upon the ZnO microcavity generate pump excitons at higher energy. The pump excitons are then scattered to form an exciton reservoir. Some

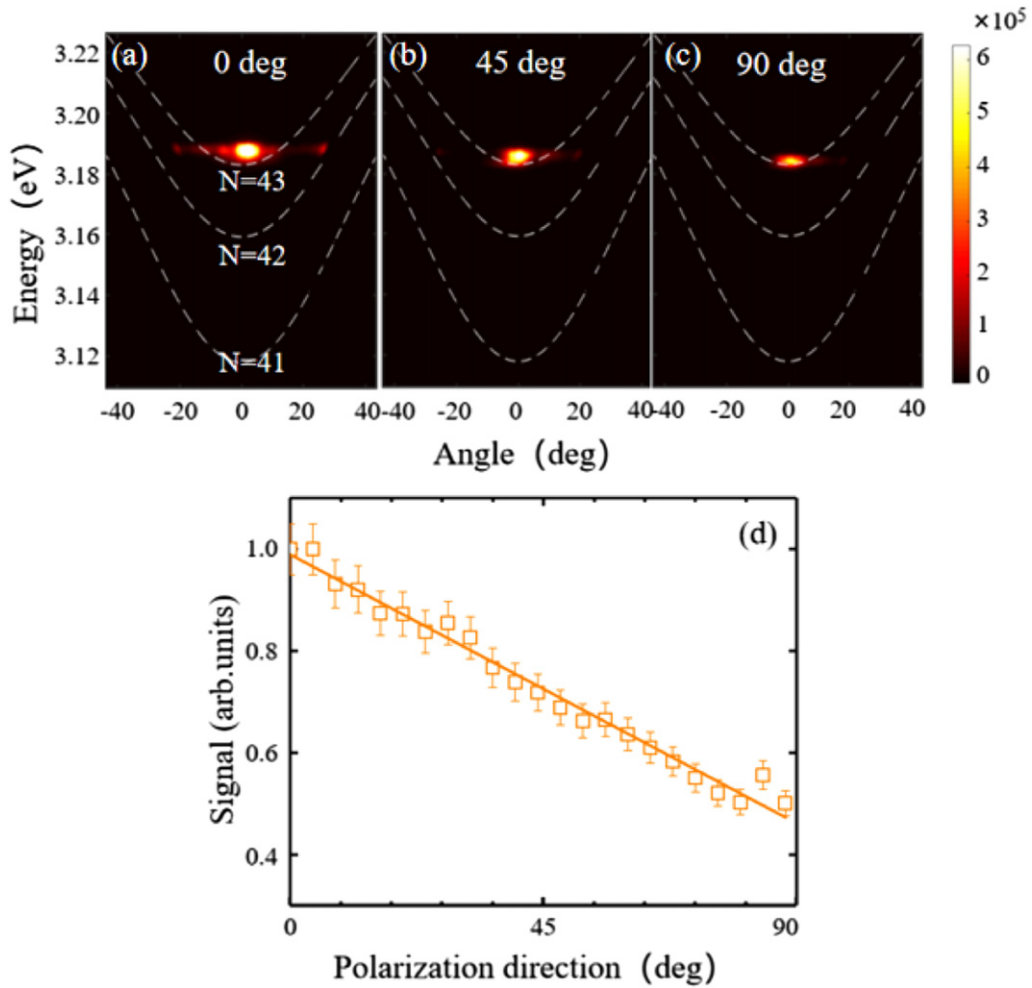


**Figure 2.** (a)–(c) Static-state  $k$ -space angle-resolved PL mappings for polariton condensates under excitation pulses along three different polarization directions. The dispersion curves (indicated by the white dashed curves) are obtained from fitting with the classical plane waves model. (d) The excitation polarization dependence of the condensation signal at a fixed pump power of  $0.8 \mu\text{W}$ . The solid line is from a linear fitting.

particles in the exciton reservoir strongly coupled with the cavity photon can generate polaritons, which relax to the bottom of a certain dispersion curve and form polariton condensates when the threshold condition is reached. The equations are written as follows.

$$\frac{\partial n_P}{\partial t} = P(x, t) - \gamma_P n_P - r n_P n_R \quad (1)$$

$$\frac{\partial n_R}{\partial t} = r n_P - \gamma_R n_R - R_1 n_R (n_1 + 1) \quad (2)$$

$$\frac{\partial n_1}{\partial t} = -\gamma_1 n_1 + R_1 n_R (n_1 + 1) \quad (3)$$

Here,  $P(t)$  indicates the pump power.  $n_P$ ,  $n_R$ , and  $n_1$  represent the densities for the pump exciton, the exciton reservoir, and the polaritons, respectively.  $\gamma_P$ ,  $\gamma_R$ ,  $\gamma_1$  are the corresponding decay rates.  $r$  and  $R_1$  are the scattering rates from the pump exciton to the exciton reservoir, and from the exciton reservoir to the EPs, respectively. The numerically simulated results are shown explicitly by the solid curves in figure 3(f). The simulation results can reproduce the main features of the experimental data to a large extent. For a fixed pumping power, the rising

of polariton condensates signals appear successively for excitation polarization directions at 0, 30, 60 and 90 degree, respectively. The most intense condensation signals are at around 7.96 ps, 9.12 ps, 10.43 ps, and 12.52 ps. Compared with the case obtained at 0 degree polarization, the condensation process at 90 degree lags by about 4.56 ps. Moreover, the lifetimes extend for polarizations at larger polarization angles. Through the exponential fitting of the relaxation process of condensation for various polarization directions, the polariton lifetimes are extracted to be 1.76 (0 degree), 2.02 (30 degree), 2.43 (60 degree), and 2.72 ps (90 degree), respectively. All these phenomena demonstrate that when the excitation laser pulses are polarized perpendicular to the  $c$ -axis of the ZnO microwire, the most efficient injection of polariton condensates can be realized. However, when the polarization is rotated towards the parallel direction with respect to the  $c$ -axis and by fixing the excitation strength, the injected polariton density becomes less and less, which is embodied in the reduction of the condensation signal, the ascending threshold, and the extended dynamics of the polariton condensates towards longer time scales.

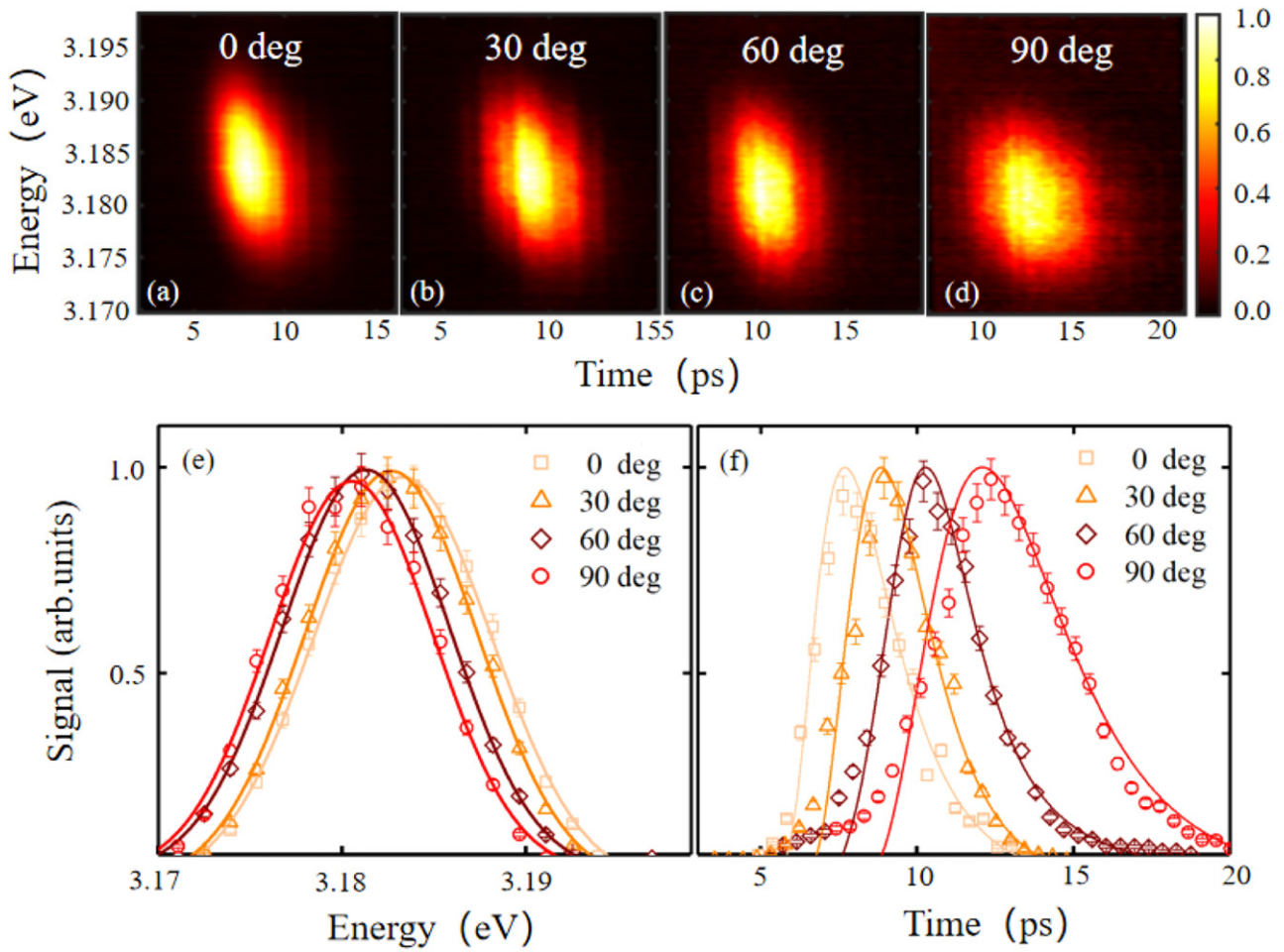


**Figure 3.** (a)–(d) The PL emission of the polariton condensation as a function of energy and time. (e) The signal are projected onto the energy axis for various polarization directions. The solid curves are fit with Gaussian function. (f) The dynamics of polariton condensation for various polarization directions. The solid curves are the calculation results based on rate equations. For a better quality of the figure, only 10% of the measured data points are shown here.

The excitation polarization dependence of polariton dynamics is explicitly measured under a series of pump powers and the results are shown in figure 4. The polarization dependence under each pump power shows similar tendency compared to the results presented in figure 3, such that the whole dynamics of the polariton condensates lags for polarization directions rotating away from the 0 degree. With the increase of the pump power, the overall polaritonic dynamics become faster, manifesting as the curves getting closer to each other on the time axis. As can be seen in figure 4, when the pump power increases from 0.80 to 1.10  $\mu\text{W}$ , the time intervals of the condensation signal between 0 degree and 90 degree polarization directions are 6.70 ps, 3.76 ps and 2.37 ps, respectively. These indicate that the effective excitation power for the various polarization direction is different within the ZnO microcavity.

The observed excitation polarization dependence could be attributed to two reasons. Considering sending a beam of femtosecond pulses onto a ZnO microwire, the effective reflectivity and coupling efficiency could be different for various polarization directions. Applying the finite element analysis method, we simulate the electric field distribution when pulses

with different polarization directions incident normally on the ZnO microwire (as schematically shown in figure 1) [25, 26]. We find that the incidence polarization direction affects the distribution of electric field inside and outside the microcavity. When the polarization direction rotates from 0 to 90 degree, the effective reflectance in the microcavity increases, resulting in an enhancement of the light field blocked out of the cavity. The summed intensity of the electric field inside the hexagonal cross section of ZnO microwire shows a decrease of about 6% when the polarization of excitation pulses changes from 0 to 90 degree, despite the fact that the actual incident powers of these cases are the same.

The other possible reason for the observed polarization dependence could be the selective excitation of distinct exciton species in ZnO microcavities. The ZnO crystal possesses wurtzite structure, with  $\Gamma_7$  symmetry for the conduction band derived from an s state, and the valence band derived from a p state. Due to the spin-orbital interaction and the field effect, the valence band can split into three energy states corresponding to three excitonic states, i.e. A- $\Gamma_9$ , B- $\Gamma_7$  and C- $\Gamma_7$ , respectively [27, 28]. The pumping polarization could result in the

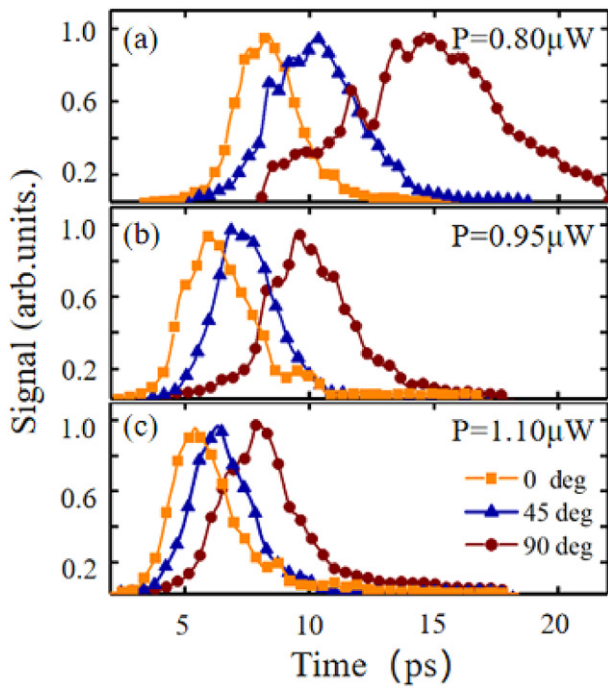


**Figure 4.** The polarization dependence of polariton condensate dynamics at pump powers of (a)  $P = 0.80 \mu\text{W}$  (b)  $P = 0.95 \mu\text{W}$  (c)  $P = 1.10 \mu\text{W}$ . As  $P$  increasing, the time interval shrinks. For a better quality of the figure, only 10% of the measured data points are shown here.

excitation of different excitons. Recently, polarization dependence in the exciton–photon coupling below the condensation threshold has been reported [29]. Based on the selection rules, for the  $\sigma$  polarization configuration (with both the polarization and the wave vector perpendicular to the  $c$  axis, i.e. the 0 degree polarization in our work), transition can occur for all the three species of excitons, where the transition probability is large for the A and B excitons but smaller for the C exciton. However, for the  $\pi$  polarization configuration (with the polarization parallel to  $c$  axis and the wave vector perpendicular to the  $c$  axis, i.e. the 90 degree polarization), transition is forbidden for the A excitons, but allowed for the B and C excitons [28]. Moreover, these three types of excitons have different preferences with cavity modes. For instance, A and B excitons prefer to interact with TE cavity modes forming TE polarized EPs. And C excitons like to interact with the transverse magnetic (TM) cavity modes (polarizing parallel to the  $c$  axis), forming TM EPs [24]. In the ZnO microcavity used in the present work, polariton condensates prefer to form in the TE modes under the nonresonant excitations [6]. All the measured data presented are obtained for the TE mode emission. As a result the signal detected is mainly from the A and B excitons. Comparing to other excitation polarization directions, there is the highest transition probability of the A and B excitons for the polarization along 0 degree. The corresponding TE mode polariton condensates show the highest density. Besides, the nonlinear interaction between particles is the strongest, contributing to the fastest dynamic process.

On the contrary, for the 90 degree polarization, the transition for the A exciton is forbidden, meanwhile, the transition probability of the B exciton is weak, thus the condensation signal is the lowest. The combined effect of these two reasons leads to the excitation polarization dependence of EPs.

On the other hand, it is found that various resonance modes (such as whispering gallery mode (WGM) and quasi-WGM) can be excited in our sample [30]. The optical paths in the cavity could be dramatic different for distinct modes, therefore the excitation polarization dependent dynamic behavior of polariton condensates may also be affected. This should be explored in the future in the ZnO microwires with varied diameter or length.

#### 4. Conclusions

In conclusion, we have investigated the excitation polarization dependence of polariton condensates in a ZnO WG microcavity at room temperature. Both the static-state and the dynamical  $k$ -space angular distributions of polariton condensates are measured explicitly. It is found that the pumping pulses with polarization direction perpendicular to the ZnO microwire is the most efficient to inject polariton condensates, where the condensates have the maximum density, the minimum pumping power threshold and the fastest dynamics. When rotating the polarization direction parallel to the  $c$ -axis, such preponderance gradually diminish. The induced polariton dynamics can be numerically reproduced by calculations based on rate equations, indicating a gradual decrease in the ground-state occupancy as the polarization direction rotates from 0 to 90 degree. The observed excitation polarization dependence can be attributed to two reasons. One is that the ZnO WG microcavity exhibits different responses to the incident laser pulses with different polarization directions. The other possible reason is the selective excitation of distinct exciton species in ZnO microcavities under different polarization directions. The revealed mechanism can deepen our understanding about the polariton dynamics at room temperature, which has shown great significance in the development of applicable polaritonic devices.

#### Acknowledgments

This work is supported by the National Key R & D Program of China (Grant Nos. 2018YFA0306303, 2018YFA0306304, 2021YFA1200803); the National Natural Science Fund (Grant Nos. 92050105, 91950201, 11834004, 11674069 and 11574205); the project supported by the Shanghai Committee of Science and Technology, China (Grant Nos. 22ZR1419700, 19ZR1473900, 19JC1412200); the NSFC Grant No. 12174111; Shanghai Municipal Science and Technology Major Project; Shanghai Pujiang Program Grant No. 21PJ1403000, and Joint Physics Research Institute Challenge Grant of the NYU-ECNU Institute of Physics at NYU Shanghai.

## Conflict of interest

We have no conflict of interest for this work to be declared.

## Data availability statement

The data that support the findings of this study are available upon reasonable request from the authors.

## ORCID iDs

Ziyu Ye  <https://orcid.org/0000-0002-2653-5025>  
Fei Chen  <https://orcid.org/0000-0001-6239-0225>  
Fenghao Sun  <https://orcid.org/0000-0003-0210-5204>  
Xianfeng Chen  <https://orcid.org/0000-0003-3025-9729>  
Jian Wu  <https://orcid.org/0000-0002-1318-2291>

## References

- [1] Anderson M H, Ensher J R, Matthews M R, Wieman C E and Cornell E A 1995 *Science* **269** 198–201
- [2] van Vugt L K, Rühle S, Ravindran P, Gerritsen H C, Kuipers L and Vanmaekelbergh D 2006 *Phys. Rev. Lett.* **97** 147401
- [3] Deng H, Haug H and Yamamoto Y 2010 *Rev. Mod. Phys.* **82** 1489–537
- [4] Amo A *et al* 2009 *Nature* **457** 291–5
- [5] Byrnes T, Kim N Y and Yamamoto Y 2014 *Nat. Phys.* **10** 803–13
- [6] Kasprzak J *et al* 2006 *Nature* **443** 409–14
- [7] Lagoudakis K G, Wouters M, Richard M, Baas A, Carusotto I, André R, Dang L S and Deveaud-Plédran B 2008 *Nat. Phys.* **4** 706–10
- [8] Xu D *et al* 2014 *Appl. Phys. Lett.* **104** 082101
- [9] Luo S, Wang Y, Liao L, Zhang Z, Shen X and Chen Z 2020 *J. Appl. Phys.* **127** 025702
- [10] Berger B, Schmidt D, Ma X, Schumacher S, Schneider C, Höfling S and Aßmann M 2020 *Phys. Rev. B* **101** 245309
- [11] Dominici L *et al* 2015 *Nat. Commun.* **6** 8993
- [12] Alves H, Pfisterer D, Zeuner A, Riemann T, Christen J, Hofmann D M and Meyer B K 2003 *Opt. Mater.* **23** 33–7
- [13] Bagnall D M, Chen Y F, Zhu Z, Yao T, Shen M Y and Goto T 1998 *Appl. Phys. Lett.* **73** 1038–40
- [14] Boemare C, Monteiro T, Soares M J, Guilherme J G and Alves E 2001 *Physica B* **308–310** 985–8
- [15] Gil B 2001 *Phys. Rev. B* **64** 201310
- [16] Teke A, Özgür Ü, Doğan S, Gu X, Morkoç H, Nemeth B, Nause J and Everitt H O 2004 *Phys. Rev. B* **70** 195207
- [17] Duan Q *et al* 2013 *Appl. Phys. Lett.* **103** 022103
- [18] Özgür Ü, Alivov Y I, Liu C, Teke A, Reshchikov M A, Doğan S, Avrutin V, Cho S-J and Morkoç H 2005 *J. Appl. Phys.* **98** 041301
- [19] Huang M H, Mao S, Feick H, Yan H, Wu Y, Kind H, Weber E, Russo R and Yang P 2001 *Science* **292** 1897–9
- [20] Paskov P P, Paskova T, Holtz P O and Monemar B 2004 *Phys. Status Solidi a* **201** 678–85
- [21] Shelykh I A, Rubo Y G, Malpuech G, Solnyshkov D D and Kavokin A 2006 *Phys. Rev. Lett.* **97** 066402
- [22] Chen F *et al* 2021 *J. Phys.: Condens. Matter* **34** 024001
- [23] Xie W, Dong H, Zhang S, Sun L, Zhou W, Ling Y, Lu J, Shen X and Chen Z 2012 *Phys. Rev. Lett.* **108** 166401
- [24] Sun L, Chen Z, Ren Q, Yu K, Bai L, Zhou W, Xiong H, Zhu Z Q and Shen X 2008 *Phys. Rev. Lett.* **100** 156403
- [25] Wiersig J 2003 *Phys. Rev. A* **67** 023807
- [26] Hu T, Xie W, Wu L, Wang Y, Zhang L and Chen Z 2017 *Solid State Commun.* **262** 7–10
- [27] Reynolds D C, Look D C, Jogai B, Litton C W, Cantwell G and Harsch W C 1999 *Phys. Rev. B* **60** 2340–4
- [28] Birman J L 1959 *Phys. Rev. Lett.* **2** 157–9
- [29] Wei H, Song J, Guo Y, Yuan X and Ren J 2022 *Opt. Commun.* **511** 128014
- [30] Zhao D, Liu W, Zhu G, Zhang Y, Wang Y, Zhou W, Xu C, Xie S and Zou B 2020 *Nano Energy* **78** 105202